

Provided for non-commercial research and education use.
Not for reproduction, distribution or commercial use.



This article appeared in a journal published by Elsevier. The attached copy is furnished to the author for internal non-commercial research and education use, including for instruction at the authors institution and sharing with colleagues.

Other uses, including reproduction and distribution, or selling or licensing copies, or posting to personal, institutional or third party websites are prohibited.

In most cases authors are permitted to post their version of the article (e.g. in Word or Tex form) to their personal website or institutional repository. Authors requiring further information regarding Elsevier's archiving and manuscript policies are encouraged to visit:

<http://www.elsevier.com/copyright>



Contents lists available at ScienceDirect

Journal of Non-Newtonian Fluid Mechanics

journal homepage: www.elsevier.com/locate/jnnfm

Observability of viscoelastic fluids

Hong Zhou^{a,*}, Wei Kang^a, Arthur Krener^a, Hongyun Wang^b^a Department of Applied Mathematics, Naval Postgraduate School, Monterey, CA 93943-5216, United States^b Department of Applied Mathematics and Statistics, University of California, Santa Cruz, CA 95060, United States

ARTICLE INFO

Article history:

Received 27 October 2009

Received in revised form 28 January 2010

Accepted 29 January 2010

Keywords:

Observability

Observability rank condition

Unscented Kalman filter

Viscoelastic models

ABSTRACT

We apply the observability rank condition to study the observability of various viscoelastic fluids under imposed shear or extensional flows. In this paper the observability means the ability of determining the viscoelastic stress from the time history of the observations of the first normal stress difference. We consider four viscoelastic models: the upper convected Maxwell (UCM) model, the Phan–Thien–Tanner (PTT) model, the Johnson–Segalman (JS) model and the Giesekus model. Our study reveals that all of the four models have observability for all stress components almost everywhere under shear flow whereas under extensional flow most of the models have no observability for the shear stress component. More specifically, for UCM and JS models under imposed shear flow, the observations of the first normal stress difference allow the reconstruction of all components of viscoelastic stress. For UCM and JS models under extensional flow, the two normal stress components can be determined from the measurements of the first normal stress difference; the shear stress component does not affect the evolution of the normal stress components and consequently it cannot be extracted from the observations. Under shear flow, the PTT and Giesekus models have observability almost everywhere. That is, all components of the viscoelastic stress can be determined from the observations when the vector formed by the components of viscoelastic stress does not lie on a certain surface. Under extensional flow, the PTT model has observability almost everywhere for normal stress components whereas the Giesekus model has observability almost everywhere for all stress components. We also run simulations using the unscented Kalman filter (UKF) to reconstruct the viscoelastic stress from observations without and with noises. The UKF yields accurate and robust estimates for the viscoelastic stress both in the absence and in the presence of observation noises.

Published by Elsevier B.V.

1. Introduction

Controllability and observability are two of the basic questions in control theory [5,11]. Formally, controllability denotes the ability of steering a system from a given initial state to a desirable final state; whereas observability is the ability to determine uniquely the state of the system from observable quantities.

The controllability of viscoelastic fluids under shear flow was studied in [12–14] and the controllability of viscoelastic fluids under other flow fields was investigated in [15,16]. Relatively little research has been conducted on the observability of viscoelastic fluids. However, observability is a very important concept in control theory since it measures how well internal states of a dynamical system can be inferred by knowledge of its external outputs. In practice, noise may appear in both the observations and the sys-

tem dynamics. If the system is not observable, then we will not be able to get an accurate estimate of the state, which will definitely reduce (if not completely destroy) our ability to guide the system to a desirable final state. Therefore, it is critical to study the observability of a dynamical system.

In this paper we extend our previous works to address the observability of viscoelastic fluids. We are following earlier work on Eulerian and Lagrangian observability of point vortex flows found in Krener [8]. In all the models considered here, we impose the velocity field and assume the viscoelastic stress is homogeneous. We assume the first normal stress difference is measured in experiments. Our goal is to infer the full viscoelastic stress. The first normal stress difference is an important rheological property of complex fluids. Common experimental devices of measuring the first normal stress difference include cone-and-plate as well as parallel-plate rheometers [3,6,10]. It is also possible to obtain values of the first normal stress difference using hole and exit pressure data [1].

We apply the observability rank condition to study short-time local observability of various models from the measurement of the first normal stress difference. The mathematical advantage of using

* Corresponding author at: Department of Applied Mathematics, Naval Postgraduate School, 833 Dyer Road, Bldg. 232, SP-250, Monterey, CA 93943-5216, United States.

E-mail address: hzhou@nps.edu (H. Zhou).

the observability rank condition is that it is simply algebraic and systematic and it also provides a tool to study more complicated systems. To the best of our knowledge, this work is the first attempt to study the observability of complex fluids.

The outline of this work is as follows. Section 2 gives a brief overview of the observability of dynamical systems and the observability rank condition. Sections 3–6 are devoted to the analysis on the observability of various viscoelastic models under shear or extensional flow by applying the observability rank condition. Section 7 presents some numerical experiments where the performance of the unscented Kalman filter is examined both in the case of zero observation noise and in the case of Gaussian observation noise. The main results of our study are summarized in Section 8. Mathematical details of the unscented Kalman filtering are included in Appendix A.

2. Observability rank condition of dynamical systems

For reader's convenience, we quickly outline the observability of dynamical systems and observability rank condition. In the subsequent sections we will investigate the observability of several viscoelastic models using the mathematical tools introduced in this section.

Consider the following system without a control input

$$\dot{x} = f(x), \quad x \in R^n \tag{1}$$

$$y = h(x), \quad y \in R^p \tag{2}$$

$$x(0) = x^0, \tag{3}$$

where x is the state variable, y is the quantity that can be observed experimentally and relation (2) is called an observation equation. We shall assume f and h are sufficiently smooth functions. The state x is not observed directly but the output y is. Can we determine the initial state x^0 from the output history $y(0 : \infty)$? In this definition, the symbol $y(0 : T)$ represents the trajectory $t \rightarrow y(t)$ where $0 \leq t < T$. Is the map $x^0 \rightarrow y(0 : \infty)$ one to one? If so, then mathematically we can reconstruct x^0 from $y(0 : \infty)$ and we say the system (1)–(2) is observable. Note that $x(t)$ can be viewed as the initial state for evolution beyond time t . Therefore, the observability also implies that $x(t)$ can be calculated from $y(0 : \infty)$.

There are other possible definitions of observability. For example, the system (1)–(2) is short-time observable if for every $T > 0$ the map $x^0 \rightarrow y(0 : T)$ is one to one. In other words, the effect of the initial data is immediately felt by the system. The system is *short-time locally observable* if for every $T > 0$, the map $x^0 \rightarrow y(0 : T)$ is locally one to one. Locally one to one means that around each x^0 there is a neighborhood such that the map is one to one on the neighborhood. More specially, locally one to one means that given any x^0 , there is a neighborhood $U(x^0)$ such that if $x^1 \in U(x^0)$, then output from x^1 is different from that from x^0 . short-time locally observable is the most useful and easiest to measure. How do we decide whether a system is short-time locally observable? In the following we review a sufficient condition for the short-time local observability [8].

First, we need to introduce some notations. Note that from (2) and (3) we have $y(0) = h(x^0)$ and thus

$$\frac{dy}{dt}(0) = \frac{\partial h}{\partial x}(x^0)f(x^0) \tag{4}$$

using the chain rule and (1). The right hand side of (4) is called the Lie derivative of the function h by the vector field f :

$$L_f(h)(x) = \frac{\partial h}{\partial x}(x)f(x). \tag{5}$$

Notice that the Lie derivative is another function from R^n to R^p , so we can repeat the process of taking the Lie derivative:

$$L_f^2(h)(x) = L_f(L_f(h))(x) = L_f\left(\frac{\partial h}{\partial x}(x)f(x)\right)$$

$$L_f^k(h)(x) = L_f(L_f^{k-1}(h))(x).$$

Definition 2.1. $g_1(x), \dots, g_k(x)$ separate points if given any pair of two points x^0 and x^1 , there is at least one $g_i(x)$ such that $g_i(x^0) \neq g_i(x^1)$.

If $g_1(x), \dots, g_k(x)$ separate points, then $x \rightarrow \begin{pmatrix} g_1(x) \\ \vdots \\ g_k(x) \end{pmatrix}$ is one to one. Mathematically, if the functions

$L_f^j(h)(x), j = 0, \dots, k$, locally separate (or distinguish) points in R^n for some k , then the system is short-time locally observable. A sufficient condition for this to happen is that the one forms

$$dh_i(x), \dots, dL_f^k(h_i)(x), \quad i = 1, \dots, p$$

span n dimensions at every x where

$$dh_i(x) = \sum_{j=1}^n \frac{\partial h_i}{\partial x_j}(x) dx_j = \left(\frac{\partial h_i}{\partial x_1}, \dots, \frac{\partial h_i}{\partial x_n} \right). \tag{6}$$

Definition 2.2. The system (1)–(2) satisfies the observability rank condition at x^0 if there exists a k such that $\left\{ dL_f^j(h_i) : j = 0, \dots, k; i = 1, \dots, p \right\}$ has rank n . The system (1)–(2) satisfies the observability rank condition if it satisfies it at every $x \in R^n$ (note k may vary with x).

For linear systems, observability rank condition (ORC) implies global short-time observability. For nonlinear systems, ORC is a sufficient condition of short-time local observability. Furthermore, ORC is almost necessary for short-time local observability. Hermann and Krener [4] have proved that if the ORC is violated on an open subset of R^n , then the system (1)–(2) is not short-time locally observable.

3. The upper convected Maxwell (UCM) model

In this section we start with simple linear models. Then we extend the analysis to nonlinear cases in the following sections.

A simple theory for viscoelasticity was proposed by Maxwell in 1867 [2,9] and has been usually called the upper convected Maxwell model. For all the models considered in this paper, we posit the velocity field and consider only the equation for the stress tensor. In this setting, the UCM model is linear and the UCM constitute equation can be written in the form

$$\dot{\mathbf{T}} - (\nabla \mathbf{v})\mathbf{T} - \mathbf{T}(\nabla \mathbf{v})^T + \lambda \mathbf{T} = 2\mu \mathbf{D}, \tag{7}$$

where \mathbf{T} is the stress tensor, \mathbf{v} is the velocity, $\nabla \mathbf{v}$ is the velocity gradient tensor, λ is the relaxation rate, μ is the elastic modulus and \mathbf{D} is the rate-of-deformation tensor (i.e. the symmetric part of the velocity gradient). In the more complicated case where the velocity field is affected by the stress tensor, we have a joint evolutionary system for the velocity field and the stress tensor, which is nonlinear. In this paper we will focus on the linear case where the velocity field is imposed.

For simplicity we restrict our attention to two-dimensional homogeneous viscoelastic fluids. We denote the stress tensor by

$$\mathbf{T} = \begin{bmatrix} T_{11} & T_{12} \\ T_{12} & T_{22} \end{bmatrix}. \tag{8}$$

The state of the system (7) is characterized by viscoelastic stress \mathbf{T} with three components T_{11} , T_{22} and T_{12} .

Now we investigate the short-time local observability of complex fluids governed by the Maxwell equation under two different simple flow conditions: extensional flow and shear flow.

3.1. UCM under extensional flow

The velocity field of a homogeneous extensional flow with rate Pe can be written as

$$\mathbf{v} = \frac{Pe}{2}(x, -y), \quad (9)$$

so the velocity gradient and the rate-of-deformation tensor both have a diagonal form:

$$\nabla \mathbf{v} = \frac{Pe}{2} \begin{bmatrix} 1 & 0 \\ 0 & -1 \end{bmatrix}, \quad (10)$$

$$\mathbf{D} = \frac{1}{2}[\nabla \mathbf{v} + (\nabla \mathbf{v})^T] = \frac{Pe}{2} \begin{bmatrix} 1 & 0 \\ 0 & -1 \end{bmatrix}. \quad (11)$$

With these simplifications (7) can be expressed as

$$\begin{aligned} \dot{T}_{11} - (Pe - \lambda)T_{11} &= \mu Pe, \\ \dot{T}_{12} + \lambda T_{12} &= 0, \\ \dot{T}_{22} + (Pe + \lambda)T_{22} &= -\mu Pe. \end{aligned} \quad (12)$$

Note that the evolution of T_{11} and T_{22} is independent of T_{12} . So we study the subsystem governing the evolution of T_{11} and T_{22} :

$$\begin{aligned} \dot{T}_{11} - (Pe - \lambda)T_{11} &= \mu Pe, \\ \dot{T}_{22} + (Pe + \lambda)T_{22} &= -\mu Pe. \end{aligned} \quad (13)$$

It is convenient to introduce the following vector

$$\bar{\mathbf{x}} = \begin{bmatrix} x_1 \\ x_2 \end{bmatrix} = \begin{bmatrix} T_{11} \\ T_{22} \end{bmatrix}.$$

This enables us to rewrite the system (13) as

$$\frac{d\bar{\mathbf{x}}}{dt} = \bar{\mathbf{f}}(\bar{\mathbf{x}}) = \begin{bmatrix} f_1 \\ f_2 \end{bmatrix} = \begin{bmatrix} -\lambda x_1 + Pe(\mu + x_1) \\ -\lambda x_2 - Pe(\mu + x_2) \end{bmatrix}. \quad (14)$$

Since the first normal stress difference $N_1 \equiv T_{11} - T_{22}$ can be measured experimentally [9], we assume that the observation is the difference of T_{11} and T_{22} , $h = T_{11} - T_{22} = x_1 - x_2$. The Lie bracket is

$$\begin{aligned} L_{\bar{\mathbf{f}}} h &= \frac{\partial h}{\partial x_i}(\bar{\mathbf{x}}) f_i(\bar{\mathbf{x}}) = \left[\frac{\partial h}{\partial x_1}, \frac{\partial h}{\partial x_2} \right] \begin{bmatrix} f_1 \\ f_2 \end{bmatrix} \\ &= [1, -1] \begin{bmatrix} f_1 \\ f_2 \end{bmatrix} \\ &= f_1 - f_2 = 2\mu Pe + (Pe - \lambda)x_1 + (Pe + \lambda)x_2. \end{aligned} \quad (15)$$

Consequently we have

$$\frac{\partial}{\partial \bar{\mathbf{x}}} \begin{bmatrix} h(\bar{\mathbf{x}}) \\ L_{\bar{\mathbf{f}}} h \end{bmatrix} = \begin{bmatrix} 1 & -1 \\ Pe - \lambda & Pe + \lambda \end{bmatrix}. \quad (16)$$

Since the determinant of this matrix is $2Pe \neq 0$, the observability rank condition is satisfied. Therefore, the subsystem of UCM model under extensional flow is short-time locally observable. In other words, when the observation is $T_{11} - T_{22}$, then T_{11} and T_{22} can be reconstructed from the observed values of $T_{11} - T_{22}$. However, T_{12} cannot be determined from the observation of $T_{11} - T_{22}$ since T_{12} does not affect the evolution of T_{11} and T_{22} at all.

3.2. UCM under shear flow

The velocity field of a shear flow with rate Pe is described by

$$\mathbf{v} = Pe(y, 0) \quad (17)$$

The rate-of-strain tensor is

$$\mathbf{D} = \frac{1}{2}[\nabla \mathbf{v} + (\nabla \mathbf{v})^T] = \frac{Pe}{2} \begin{bmatrix} 0 & 1 \\ 1 & 0 \end{bmatrix}. \quad (18)$$

The UCM model (7) becomes

$$\begin{aligned} \dot{T}_{11} - 2Pe T_{12} + \lambda T_{11} &= 0, \\ \dot{T}_{12} - Pe T_{22} + \lambda T_{12} &= \mu Pe, \\ \dot{T}_{22} + \lambda T_{22} &= 0. \end{aligned} \quad (19)$$

We remark that although the dynamics of T_{22} can be separated from T_{11} and T_{22} , T_{12} still affects the evolution of T_{11} and T_{22} ; and consequently T_{12} may still be recovered from observations of $T_{11} - T_{22}$, which is the case we will see below.

The system (19) can be rewritten as

$$\frac{d\bar{\mathbf{x}}}{dt} = \bar{\mathbf{f}}(\bar{\mathbf{x}}), \quad (20)$$

where

$$\bar{\mathbf{x}} = \begin{bmatrix} x_1 \\ x_2 \\ x_3 \end{bmatrix} = \begin{bmatrix} T_{11} \\ T_{12} \\ T_{22} \end{bmatrix}, \quad \bar{\mathbf{f}}(\bar{\mathbf{x}}) = \begin{bmatrix} -\lambda x_1 + 2Pe x_2 \\ -\lambda x_2 + Pe x_3 + \mu Pe \\ -\lambda x_3 \end{bmatrix}. \quad (21)$$

Assume that the quantity that can be measured is the normal stress

$$h(\bar{\mathbf{x}}) = T_{11} - T_{22} = x_1 - x_3.$$

To check the observability rank condition, we first calculate the Lie brackets:

$$\begin{aligned} L_{\bar{\mathbf{f}}} h &= \frac{\partial h \partial \bar{\mathbf{x}}}{\bar{\mathbf{f}}}(\bar{\mathbf{x}}) = [1, 0, -1] \bar{\mathbf{f}}(\bar{\mathbf{x}}) = \lambda(x_3 - x_1) + 2Pe x_2, \\ L_{\bar{\mathbf{f}}}^2 h &= L_{\bar{\mathbf{f}}}(L_{\bar{\mathbf{f}}} h) = [-\lambda, 2Pe, \lambda] \bar{\mathbf{f}}(\bar{\mathbf{x}}) \\ &= \lambda^2 x_1 - 4\lambda Pe x_2 + (2Pe^2 - \lambda^2)x_3 + 2\mu Pe^2. \end{aligned} \quad (22)$$

So

$$\frac{\partial}{\partial \bar{\mathbf{x}}} \begin{bmatrix} h \\ L_{\bar{\mathbf{f}}} h \\ L_{\bar{\mathbf{f}}}^2 h \end{bmatrix} = \begin{bmatrix} 1 & 0 & -1 \\ -\lambda & 2Pe & \lambda \\ \lambda^2 & -4\lambda Pe & 2Pe^2 - \lambda^2 \end{bmatrix}. \quad (23)$$

This matrix is nonsingular since its determinant is $4Pe^3 \neq 0$. Thus, the observability rank condition is satisfied and the Maxwell model (19) under shear flow is short-time locally observable if the observation is $T_{11} - T_{22}$. In contrast to the case of extensional flow where T_{12} does not affect the evolution of (T_{11}, T_{22}) and T_{12} cannot be determined from observed values of $T_{11} - T_{22}$, in the case of shear flow all three of T_{11} , T_{22} and T_{12} can be reconstructed from the observed values of $T_{11} - T_{22}$.

4. The Phan–Thien–Tanner (PTT) model

The Phan–Thien–Tanner model was developed from network theory to model the rheological behavior of polymer melts. It has the form

$$\dot{\mathbf{T}} - (\nabla \mathbf{v})\mathbf{T} - \mathbf{T}(\nabla \mathbf{v})^T + \lambda \mathbf{T} + \nu(\text{tr} \mathbf{T})\mathbf{T} = 2\mu \mathbf{D}, \quad (24)$$

where all the notations have the same meaning as in UCM model. In addition, the symbol “tr” denotes the trace of the tensor and ν is a constant.

4.1. PTT under extensional flow

Under extensional flow (9), the PTT model (24) can be written in vector form:

$$\frac{d\bar{x}}{dt} = \bar{f}(\bar{x}), \quad \bar{x} = \begin{bmatrix} x_1 \\ x_2 \\ x_3 \end{bmatrix} = \begin{bmatrix} T_{11} \\ T_{12} \\ T_{22} \end{bmatrix}, \tag{25}$$

and

$$\bar{f}(\bar{x}) = \begin{bmatrix} -[\lambda + \nu(x_1 + x_3)]x_1 + (\mu + x_1)Pe \\ -[\lambda + \nu(x_1 + x_3)]x_2 \\ -[\lambda + \nu(x_1 + x_3)]x_3 - (\mu + x_3)Pe \end{bmatrix} \equiv \begin{bmatrix} f_1 \\ f_2 \\ f_3 \end{bmatrix}. \tag{26}$$

Notice that the governing equations for x_1 and x_3 are given by the first and third equations in the above, which are independent of x_2 . Therefore, we first consider the observability of the subsystem consisting of two equations:

$$\frac{d}{dt} \begin{bmatrix} x_1 \\ x_3 \end{bmatrix} \equiv \frac{d}{dt} \begin{bmatrix} T_{11} \\ T_{22} \end{bmatrix} = \begin{bmatrix} -[\lambda + \nu(x_1 + x_3)]x_1 + (\mu + x_1)Pe \\ -[\lambda + \nu(x_1 + x_3)]x_3 - (\mu + x_3)Pe \end{bmatrix} \equiv \bar{f}_{new}. \tag{27}$$

Again, we assume that the observable quantity is the first normal stress difference

$$h = T_{11} - T_{22} = x_1 - x_3.$$

Then it is found that

$$\det \left(\frac{\partial}{\partial \bar{x}_{new}} \begin{bmatrix} \bar{h} \\ L_{\bar{f}_{new}} h \end{bmatrix} \right) = \det \begin{bmatrix} 1 & -1 \\ -\lambda - 2\nu x_1 + Pe & \lambda + 2\nu x_3 + Pe \end{bmatrix} = 2\nu(x_3 - x_1) + 2Pe, \tag{28}$$

where $\bar{x}_{new} = \begin{bmatrix} x_1 \\ x_3 \end{bmatrix}$. Clearly, the ORC is satisfied if $x_3 - x_1 \neq -Pe/\nu$.

Or equivalently, when the first normal stress $T_{11} - T_{22}$ does not have the value Pe/ν , then T_{11} and T_{22} are short-time locally observable. That is, T_{11} and T_{22} can be reconstructed from the observed values of $T_{11} - T_{22}$.

Now let us briefly check the observability of the whole system (25) when the observation is the first normal stress difference $T_{11} - T_{22}$. In this case, the Lie bracket is

$$L_{\bar{f}} h = [1, 0, -1] \bar{f} = f_1 - f_3.$$

Note that both f_1 and f_2 are independent of x_2 . It follows that the Lie bracket

$$L_{\bar{f}}^2 h = L_{\bar{f}}(L_{\bar{f}} h),$$

is also independent of x_2 . As a result, the second column of the 3×3 matrix

$$\frac{\partial}{\partial \bar{x}} \begin{bmatrix} h \\ L_{\bar{f}} h \\ L_{\bar{f}}^2 h \end{bmatrix}$$

is entirely made of zeros. So the observability rank condition is not satisfied and this implies that from the observation of $T_{11} - T_{22}$, it is not possible to reconstruct the whole viscoelastic stress \mathbf{T} .

In conclusion, for the PTT model under extensional flow, the observation of the first normal stress difference $T_{11} - T_{22}$ allows short-time local observability of T_{11} and T_{22} when the stress tensor is away from $T_{11} - T_{22} = Pe/\nu$. T_{12} is not observable.

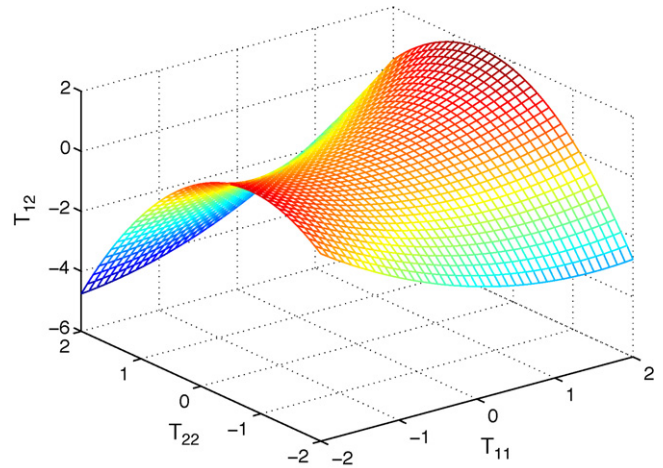


Fig. 1. The surface where the determinant in (31) is zero. The PTT model under shear is observable for all stress components when the stress tensor is away from this surface.

4.2. PTT under shear flow

In the presence of a shear flow (17), the PTT model (24) becomes

$$\frac{d\bar{x}}{dt} = \bar{f}(\bar{x}), \quad \bar{x} = \begin{bmatrix} x_1 \\ x_2 \\ x_3 \end{bmatrix} = \begin{bmatrix} T_{11} \\ T_{12} \\ T_{22} \end{bmatrix}, \tag{29}$$

and

$$\bar{f}(\bar{x}) = \begin{bmatrix} -[\lambda + \nu(x_1 + x_3)]x_1 + 2Pe x_2 \\ -[\lambda + \nu(x_1 + x_3)]x_2 + Pe x_3 + \mu Pe \\ -[\lambda + \nu(x_1 + x_3)]x_3 \end{bmatrix} \equiv \begin{bmatrix} f_1 \\ f_2 \\ f_3 \end{bmatrix}. \tag{30}$$

If the observation is

$$h = T_{11} - T_{22} = x_1 - x_3,$$

then the Lie brackets are

$$L_{\bar{f}} h = f_1 - f_3 = -\lambda x_1 - \nu x_1^2 + 2Pe x_2 + \lambda x_3 + \nu x_3^2,$$

$$L_{\bar{f}}^2 h = (-\lambda - 2\nu x_1)f_1 + 2Pe f_2 + (\lambda + 2\nu x_3)f_3.$$

After some algebraic manipulations, we obtain

$$\det \left(\frac{\partial}{\partial \bar{x}} \begin{bmatrix} \bar{h} \\ L_{\bar{f}} h \\ L_{\bar{f}}^2 h \end{bmatrix} \right) = 4Pe (Pe^2 - 4\nu Pe x_2 + \nu^2 x_1^2 - 3\nu^2 x_3^2 + \lambda \nu x_1 - \lambda \nu x_3 + 2\nu^2 x_1 x_3). \tag{31}$$

So one can conclude that the PTT model under shear (29) is short-time locally observable for all stress components if $Pe^2 - 4\nu Pe x_2 + \nu^2 x_1^2 - 3\nu^2 x_3^2 + \lambda \nu x_1 - \lambda \nu x_3 + 2\nu^2 x_1 x_3 \neq 0$.

In Fig. 1 we plot the surface described by $Pe^2 - 4\nu Pe x_2 + \nu^2 x_1^2 - 3\nu^2 x_3^2 + \lambda \nu x_1 - \lambda \nu x_3 + 2\nu^2 x_1 x_3 = 0$ where the parameters are chosen as $Pe = \nu = \lambda = 1$. So the PTT model under shear flow is short-time locally observable as long as the point (T_{11}, T_{22}, T_{12}) does not lie on the surface.

5. The Johnson–Segalman (JS) model

The Johnson–Segalman (JS) model, which allows for a non-monotonic relationship between the shear stress and shear rate, has been widely used to explain the striking “spurt” phenomenon of non-Newtonian fluids. This phenomenon describes a sudden

increase in the volumeric flow rate. The JS model is given by

$$\dot{\mathbf{T}} - \frac{a+1}{2} [(\nabla\mathbf{v})\mathbf{T} + \mathbf{T}(\nabla\mathbf{v})^T] - \frac{a-1}{2} [(\nabla\mathbf{v})^T\mathbf{T} + \mathbf{T}(\nabla\mathbf{v})] + \lambda\mathbf{T} = 2\mu\mathbf{D}. \quad (32)$$

Here a is a parameter describing polymer slip where $-1 < a < 1$; When $a = 1$, the model (32) reduces to the Oldroyd-B model.

5.1. JS under extensional flow

Applying the extensional flow (9), we can express the JS system (32) as

$$\frac{d\bar{\mathbf{x}}}{dt} = \bar{\mathbf{f}}(\bar{\mathbf{x}}), \quad \bar{\mathbf{x}} = \begin{bmatrix} x_1 \\ x_2 \\ x_3 \end{bmatrix} = \begin{bmatrix} T_{11} \\ T_{12} \\ T_{22} \end{bmatrix}, \quad (33)$$

and

$$\bar{\mathbf{f}}(\bar{\mathbf{x}}) = \begin{bmatrix} -\lambda x_1 + (\mu + ax_1)Pe \\ -\lambda x_2 \\ -\lambda x_3 - (\mu + ax_3)Pe \end{bmatrix}. \quad (34)$$

As in the upper convected Maxwell model, the component x_2 or T_{12} does not affect the evolution of T_{11} and T_{22} . So we consider the subsystem of T_{11} and T_{22} :

$$\frac{d\bar{\mathbf{x}}_{\text{new}}}{dt} = \bar{\mathbf{f}}_{\text{new}}(\bar{\mathbf{x}}) = \begin{bmatrix} -\lambda x_1 + (\mu + ax_1)Pe \\ -\lambda x_3 - (\mu + ax_3)Pe \end{bmatrix}, \quad \bar{\mathbf{x}}_{\text{new}} = \begin{bmatrix} x_1 \\ x_3 \end{bmatrix} \quad (35)$$

Assume the observation is the first normal stress difference

$$h = T_{11} - T_{22} = x_1 - x_3,$$

then it follows that

$$\frac{\partial}{\partial \bar{\mathbf{x}}} \begin{bmatrix} \bar{h} \\ L_{\bar{\mathbf{f}}_{\text{new}}} \bar{h} \end{bmatrix} = \begin{bmatrix} 1 & -1 \\ -\lambda + aPe & \lambda + aPe \end{bmatrix}, \quad (36)$$

whose determinant is the nonzero value $2aPe$. This means that the observability rank condition is satisfied. Therefore, for the JS model under extensional flow the observation of the first normal stress difference $T_{11} - T_{22}$ allows short-time local observability of T_{11} and T_{22} , but not T_{12} .

5.2. JS under shear flow

Under shear flow the JS model is described by

$$\frac{d\bar{\mathbf{x}}}{dt} = \bar{\mathbf{f}}(\bar{\mathbf{x}}), \quad \bar{\mathbf{x}} = \begin{bmatrix} x_1 \\ x_2 \\ x_3 \end{bmatrix} = \begin{bmatrix} T_{11} \\ T_{12} \\ T_{22} \end{bmatrix}, \quad (37)$$

and

$$\bar{\mathbf{f}}(\bar{\mathbf{x}}) = \begin{bmatrix} -\lambda x_1 + (a+1)Pe x_2 \\ -\lambda x_2 + \frac{a+1}{2}Pe x_3 + \frac{a-1}{2}Pe x_1 + \mu Pe \\ -\lambda x_3 + (a-1)Pe x_2 \end{bmatrix} \equiv \begin{bmatrix} f_1 \\ f_2 \\ f_3 \end{bmatrix}. \quad (38)$$

If the observation is

$$h = T_{11} - T_{22} = x_1 - x_3,$$

then the Lie brackets are

$$L_{\bar{\mathbf{f}}} h = f_1 - f_3 = -\lambda x_1 + \lambda x_3 + 2Pe x_2,$$

$$L_{\bar{\mathbf{f}}}^2 h = -\lambda f_1 + \lambda f_3 + 2Pe f_2$$

$$= [\lambda^2 + (a-1)Pe^2]x_1 - 4\lambda Pe x_2 + [-\lambda^2 + (a+1)Pe^2]x_3 + 2\mu Pe^2.$$

This leads to

$$\det \left(\frac{\partial}{\partial \bar{\mathbf{x}}} \begin{bmatrix} h \\ L_{\bar{\mathbf{f}}} h \\ L_{\bar{\mathbf{f}}}^2 h \end{bmatrix} \right) = \det \begin{bmatrix} 1 & 0 & -1 \\ -\lambda & 2Pe & \lambda \\ \lambda^2 + (a-1)Pe^2 & -4\lambda Pe & -\lambda^2 + (a+1)Pe^2 \end{bmatrix} = 4aPe^3 \neq 0. \quad (39)$$

So the observability rank condition is validated and therefore for the JS model under shear (37) the viscoelastic stress is short-time locally observable if the observation is the first normal stress difference.

6. The Giesekus model

The Giesekus model is a nonlinear viscoelastic fluid model which reproduces many characteristics of the rheology of polymer solutions as well as other liquids. It takes the form

$$\dot{\mathbf{T}} - (\nabla\mathbf{v})\mathbf{T} - \mathbf{T}(\nabla\mathbf{v})^T + \lambda\mathbf{T} + \nu\mathbf{T}^2 = 2\mu\mathbf{D}. \quad (40)$$

6.1. The Giesekus model under extensional flow

Under extensional flow (9), the Giesekus model (40) becomes

$$\frac{d\bar{\mathbf{x}}}{dt} = \bar{\mathbf{f}}(\bar{\mathbf{x}}), \quad \bar{\mathbf{x}} = \begin{bmatrix} x_1 \\ x_2 \\ x_3 \end{bmatrix} = \begin{bmatrix} T_{11} \\ T_{12} \\ T_{22} \end{bmatrix}, \quad (41)$$

and

$$\bar{\mathbf{f}}(\bar{\mathbf{x}}) = \begin{bmatrix} -\lambda x_1 - \nu(x_1^2 + x_2^2) + (\mu + x_1)Pe \\ -[\lambda + \nu(x_1 + x_3)]x_2 \\ -\lambda x_3 - \nu(x_2^2 + x_3^2) - (\mu + x_3)Pe \end{bmatrix} \equiv \begin{bmatrix} f_1 \\ f_2 \\ f_3 \end{bmatrix}. \quad (42)$$

To investigate the observability of the system (41), we assume the observation is the first normal stress difference

$$h = T_{11} - T_{22} = x_1 - x_3.$$

Then, after some calculations, we find that

$$\det \left(\frac{\partial}{\partial \bar{\mathbf{x}}} \begin{bmatrix} h \\ L_{\bar{\mathbf{f}}} h \\ L_{\bar{\mathbf{f}}}^2 h \end{bmatrix} \right) = 4\nu x_2 [\nu(x_1 - x_3) - Pe]^2. \quad (43)$$

So the observability rank condition test is valid if $x_2 \neq 0$ (i.e. $T_{12} \neq 0$) and $\nu(x_3 - x_1) + Pe \neq 0$ (i.e. $T_{11} - T_{22} \neq Pe/\nu$). That is, for the Giesekus model under extensional flow, the observation of the first normal stress difference $T_{11} - T_{22}$ gives the short-time local observability of the viscoelastic stress provided that $T_{12} \neq 0$ and $T_{11} - T_{22} \neq Pe/\nu$.

6.2. The Giesekus model under shear flow

Finally, we consider the observability of the Giesekus model under shear flow:

$$\frac{d\bar{\mathbf{x}}}{dt} = \bar{\mathbf{f}}(\bar{\mathbf{x}}), \quad \bar{\mathbf{x}} = \begin{bmatrix} x_1 \\ x_2 \\ x_3 \end{bmatrix} = \begin{bmatrix} T_{11} \\ T_{12} \\ T_{22} \end{bmatrix}, \quad (44)$$

and

$$\bar{\mathbf{f}}(\bar{\mathbf{x}}) = \begin{bmatrix} -\lambda x_1 - \nu(x_1^2 + x_2^2) + 2Pe x_2 \\ -[\lambda + \nu(x_1 + x_3)]x_2 + Pe x_3 + \mu Pe \\ -\lambda x_3 - \nu(x_2^2 + x_3^2) \end{bmatrix}. \quad (45)$$

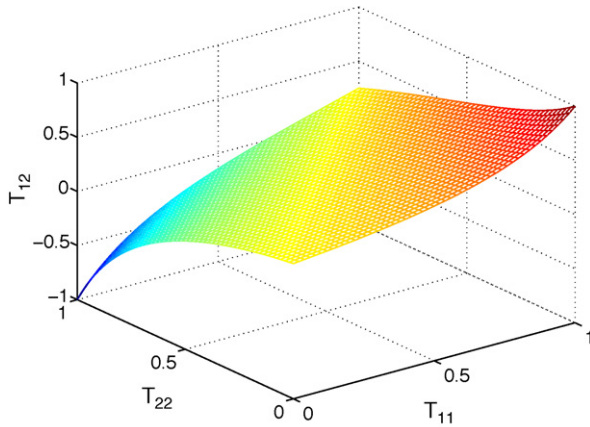


Fig. 2. The surface where the determinant in (46) vanishes. The Giesekus model under shear is observable for all stress components as long as the stress tensor is away from this surface.

As usual, assume that the observation is the first normal stress difference

$$h = T_{11} - T_{22} = x_1 - x_3.$$

Some algebra gives

$$\det \left(\frac{\partial}{\partial \bar{x}} \begin{bmatrix} h \\ L_f^1 h \\ L_f^2 h \end{bmatrix} \right) = 4Pe^3 + 4Pe\lambda\nu(x_1 - x_3) - 16\nu(\nu^2 x_1 x_3 + Pe^2)x_2 + 8\nu^2 Pe(x_1 - x_3)x_3 + 8\nu^3 x_2(x_1^2 + x_3^2). \quad (46)$$

Therefore, the Giesekus model under shear (44) is short-time locally observable if the determinant in (46) does not vanish.

Fig. 2 depicts the surface where the determinant in (46) is zero. Here we choose all the parameters to be one: $Pe = \lambda = \nu = 1$. Clearly, the Giesekus model under shear flow is short-time locally observable provided that (T_{11}, T_{22}, T_{12}) is not on this surface.

7. Unscented Kalman filtering (UKF) of complex fluids

The observability of a system tells us only the mathematical possibility of recovering the state of the system from observable quantity. It does not, however, provide us a concrete way of extract-

ing the state from observations. The most intuitive way of direct reconstruction of state is to use repeated differentiation. Unfortunately, numerical differentiation is susceptible to measurement noise. The family of Kalman filters is an efficient and robust method for reconstructing the solution without resorting to numerical differentiation. Numerical differentiation requires only data over very short time. In contrast, Kalman filters use data over a period of time to avoid the instability associated with repeated numerical differentiation. In addition, Kalman filters can deal with the case where the measurements are polluted by noise of fairly large magnitude, in which case numerical differentiation will certainly fail.

In this section we demonstrate the performance of unscented Kalman filtering in recovering the viscoelastic stress from the observed first normal stress difference. We will examine two cases: (1) the observation is noise free and (2) the observation contains Gaussian noise.

The unscented Kalman filtering was first developed by Julier et al. [7] and it has been one of the workhorses of nonlinear estimation problems. While the original Kalman filter was developed for linear systems, the idea was generalized to nonlinear systems and led to many methods for nonlinear systems, including extended Kalman filter (EKF), UKF, Ensemble Kalman filter, etc. The technique of UKF is more accurate and easier to implement than an EKF. EKF is based on the linearization of the dynamic system, which may cause numerical instability due to nonlinear effects. In addition, EKF requires deriving a Jacobian matrix which is a challenging task for complex systems. In contrast, UKF is an approach that takes into account the nonlinear dynamics, rather than its linearization, in the propagation of covariance matrix. UKF is “founded on the intuition that it is easier to approximate a probability distribution than it is to approximate an arbitrary nonlinear function or transformation” [7]. A numerical recipe for the UKF is given in Appendix A.

To test UKF for a non-steady state solution of the UCM model under shear flow, we add an external force

$$\begin{bmatrix} 0 \\ 0.5 \sin(t) \\ 0 \end{bmatrix} \quad (47)$$

to the right-hand side of the equation (20). We remark that the observability study in the previous section is still valid here since in (23) $L_f^1 h$ is unchanged whereas $\partial/\partial \bar{x} L_f^2 h$ is the same as before.

We start the system (20) with the external force (47) at some initial condition $\bar{x}(0)$ and the filter at a different initial condition $\tilde{x}(0)$. We solve the system equations without noise to get state $\bar{x}(t)$:

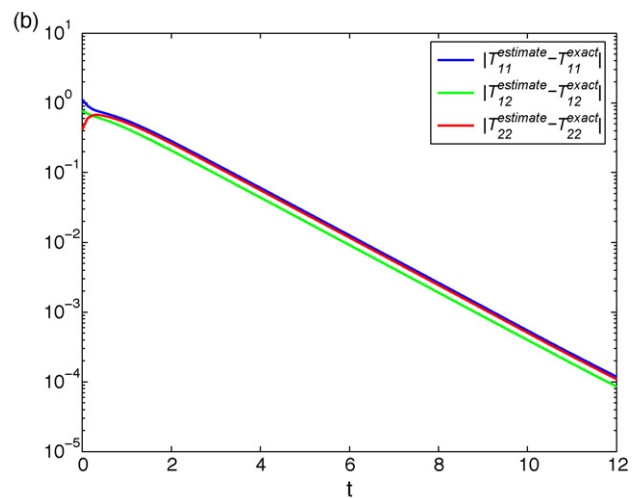
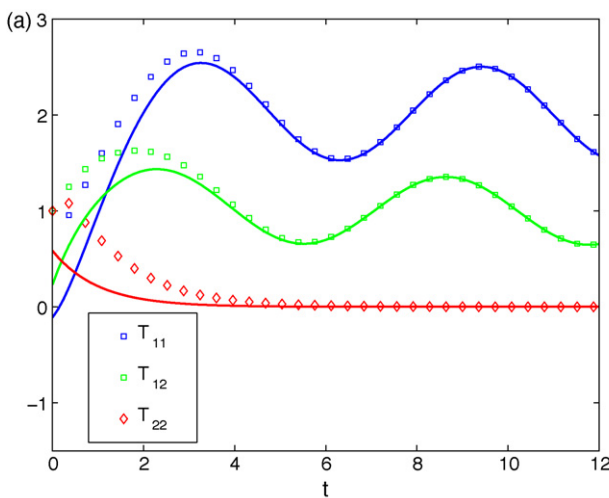


Fig. 3. (a) Exact solutions (solid lines) and estimated solutions from UKF (symbols) of UCM model under shear flow with an external force. (b) Corresponding filter errors of UKF in (a).

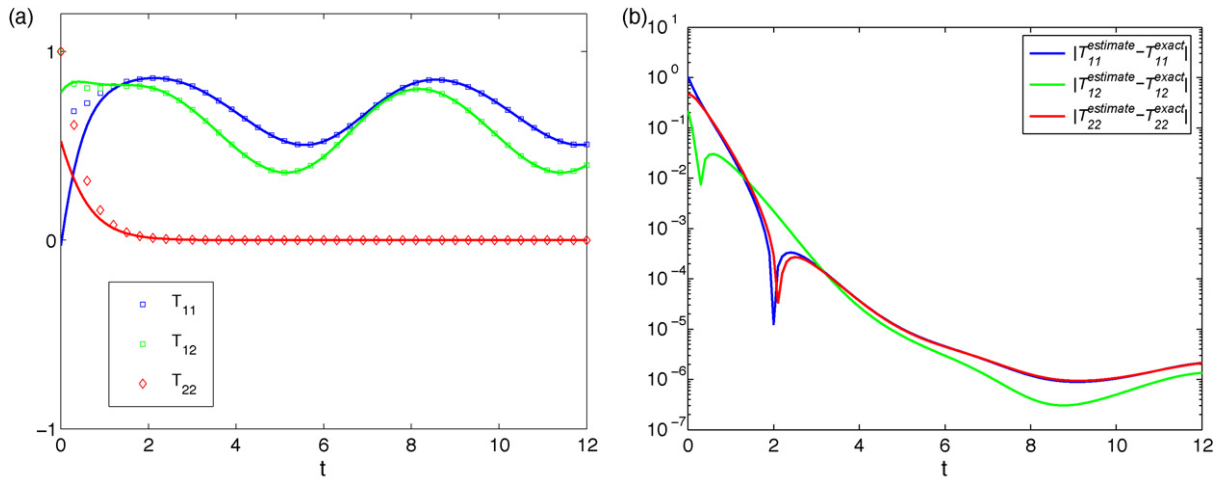


Fig. 4. (a) Exact solutions (solid lines) and estimated solutions from UKF (symbols) of PTT model under shear flow with an external force. (b) Corresponding filter errors of UKF.

∞) and observation $h(0 : \infty)$ trajectories. In the case of observations with no noise, we pass the noise free observation trajectory to the filter and the filter yields a state estimate trajectory $\hat{x}(0 : \infty)$. The estimation error $\bar{x}(t) - \hat{x}(t)$ is the difference between the state of the system (which is not directly measurable) and the estimate state

produced by the filter from the observation. The filter is said to be convergent if the estimation error goes to zero as $t \rightarrow \infty$ for any $\bar{x}(0)$ and $\hat{x}(0)$.

In Fig. 3 we show the results of UKF for the UCM model under shear flow. The parameters used here are $\lambda = 1.0$, $Pe = 1.0$, and

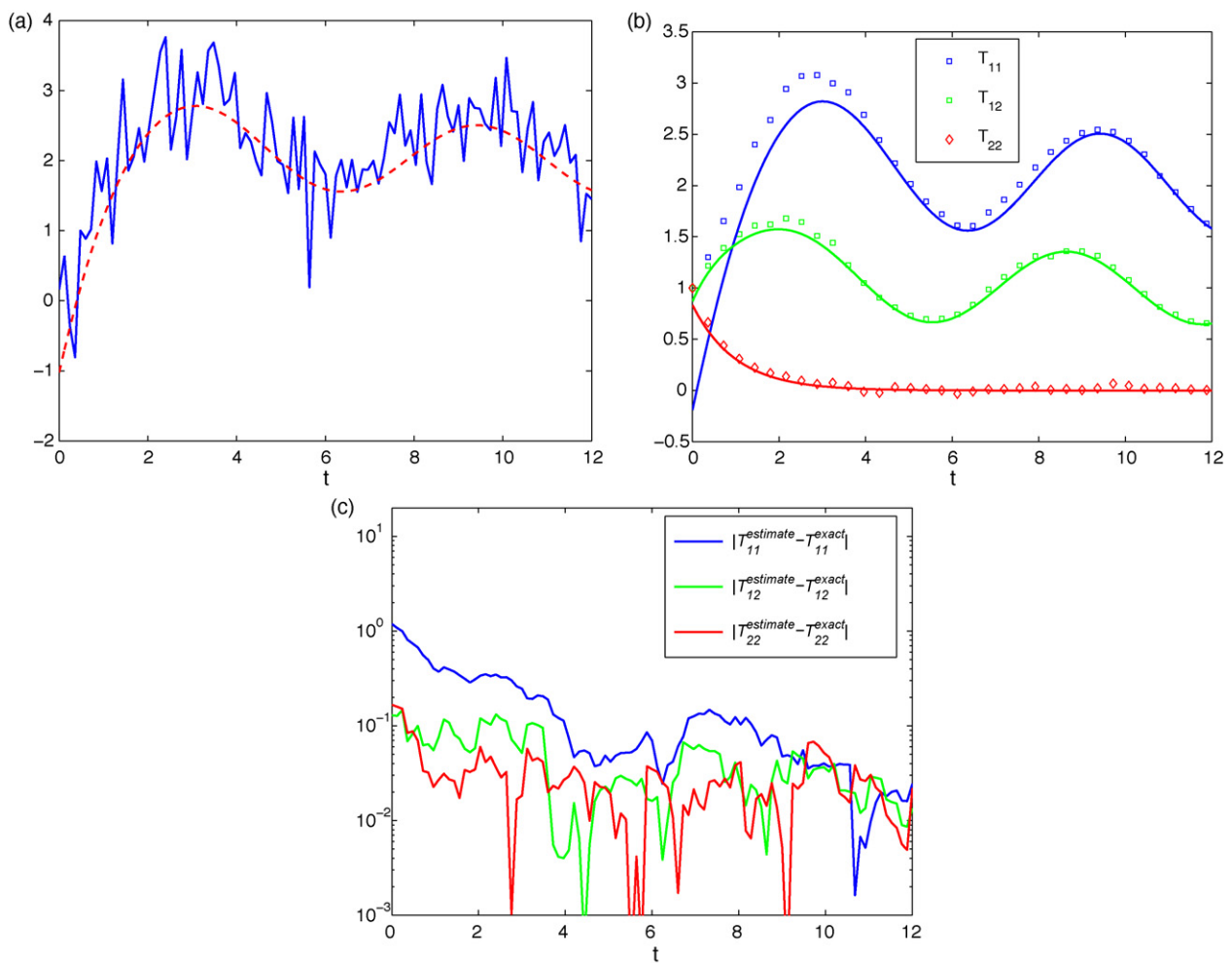


Fig. 5. (a) Observation with Gaussian noise (solid line) vs observation without noise (dashed line). (b) Exact solutions (solid lines) and estimated solutions from UKF (symbols) of UCM model under shear flow with an external force where observations contain Gaussian noise. (c) Corresponding filter errors of UKF in (b).

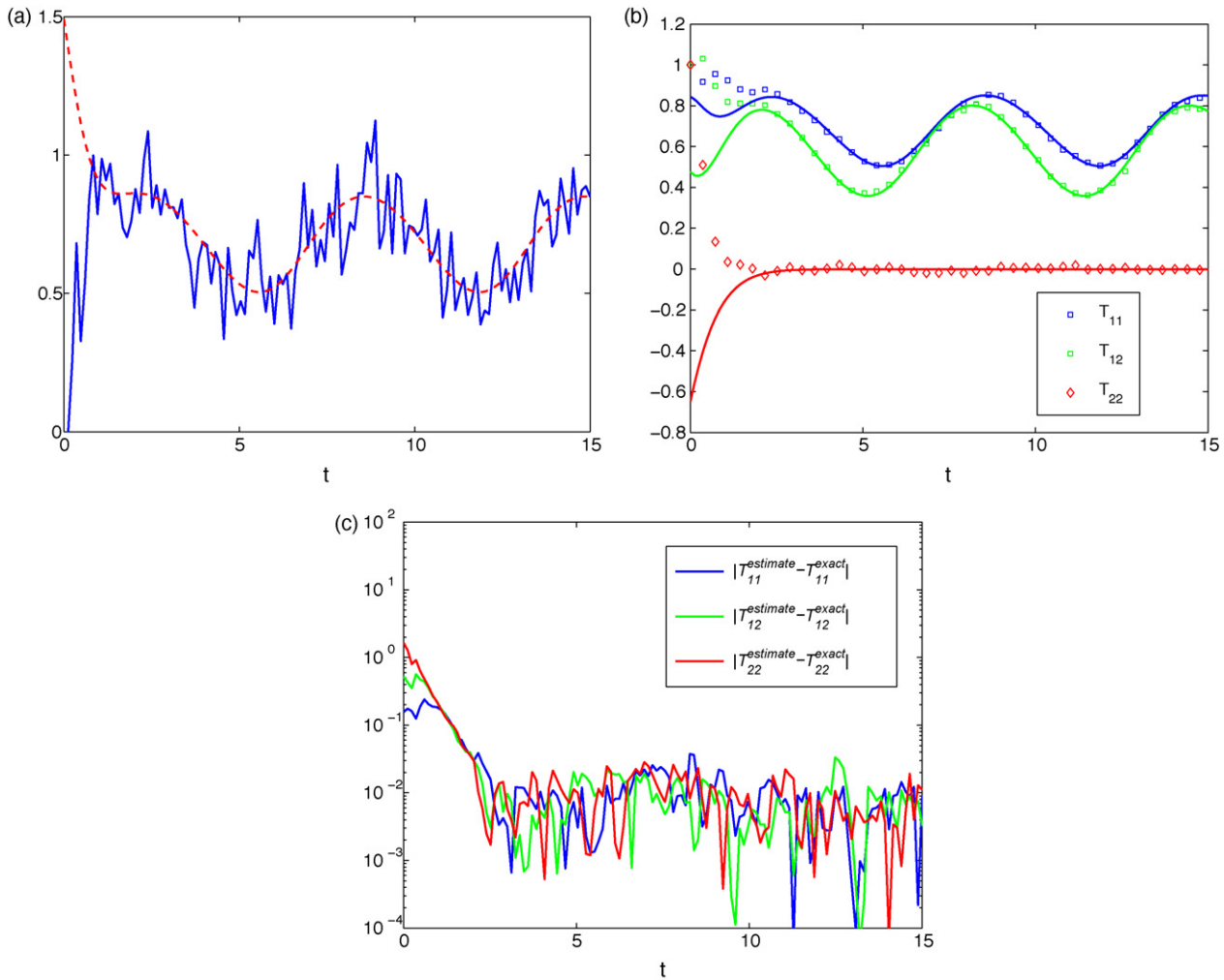


Fig. 6. (a) Observation with Gaussian noise (solid line) vs observation without noise (dashed line). (b) Exact solutions (solid lines) and estimated solutions from UKF (symbols) of PTT model under shear flow with an external force where observations contain Gaussian noise. (c) Corresponding filter errors of UKF in (b).

$\mu = 1.0$. The left panel depicts the exact and estimated solutions of the UCM system, respectively, whereas the right panel gives the corresponding errors of the estimated solutions. Fig. 3 shows the convergence of the UKF when there is no noise but only initial estimate error.

Then we carry out the simulations of the PTT model under shear flow with the external force (47) added to the system as well. Our results are plotted in Fig. 4 where the parameters are $\lambda = 1.0$, $Pe = 1.0$, $\mu = 1.0$, and $\nu = 1.0$. Again, the UKF converges in the absence of noise.

In reality all observations are polluted by noises from various sources. Next, we examine the performance of UKF in the presence of observation noise. We add Gaussian noise to the measurements. Specifically, we assume that the experimental measurement is the true value of the observation plus Gaussian noise:

$$h_{\text{experiment}}(0 : \infty) = h(0 : \infty) + \text{Gaussian noise.}$$

Then we pass the observation with noise $h_{\text{experiment}}(0 : \infty)$ to the filter. The filter outputs an estimated state. Fig. 5 shows the results of UKF for the UCM model under shear flow. Fig. 5(a) depicts the measurement with noises (the solid line) vs the measurement without noise (dashed line). The exact solutions and estimated solutions from UKF are plotted in Fig. 5(b) whereas the corresponding filter errors are given in Fig. 5(c). It is clear that UKF gives very good estimate even when noises are present in the measurements.

The performance of UKF in the presence of noise for the PTT model under shear flow is demonstrated in Fig. 6. Again, UKF gives very good estimates when the measurements contain noise. In particular, the estimation error is much smaller than the magnitude of the measurement noise.

8. Concluding remarks

In this paper we have applied the observability rank condition (ORC) to the vector fields in the various constitutive models to study the short-time local observability of complex fluids driven by extensional or shear flow fields. In each case the measurement is assumed to be the first normal stress difference $T_{11} - T_{22}$. We summarize our main results as follows.

- For the upper convected Maxwell model under extensional flow, the observation of the first normal stress difference allows the short-time local observability of the two components T_{11} and T_{22} of the viscoelastic stress, but not the component T_{12} . In contrast, for the UCM model under shear flow, the observation of the first normal stress difference leads to the short-time local observability of all components of the viscoelastic stress.
- For the Phan–Thien–Tanner model under extensional flow, the observation of the first normal stress difference provides short-time local observability of T_{11} and T_{22} , but not T_{12} , if $T_{11} -$

$T_{22} \neq Pe/\nu$. For the PTT model under shear flow, the observation of the first normal stress allows the reconstruction of viscoelastic stress as long as the stress is away from the surface prescribed by the equation

$$Pe^2 - 4\nu Pe T_{12} + \nu^2 T_{11}^2 - 3\nu^2 T_{22}^2 + \lambda \nu T_{11} - \lambda \nu T_{22} + 2\nu^2 T_{11} T_{22} = 0.$$

- For the Johnson–Segalman (JS) model under extensional flow, the observation of the first normal stress difference leads to the short-time local observability of the two components T_{11} and T_{22} of the viscoelastic stress, but not the component T_{12} . For the JS model under shear flow, the observation of the first normal stress difference gives the short-time local observability of the full viscoelastic stress.
- For the Giesekus model under extensional flow, the observation of the first normal stress difference provides the short-time local observability of the full viscoelastic stress if $T_{12} \neq 0$ and $T_{11} - T_{22} \neq Pe/\nu$. On the other hand, the Giesekus model under shear flow is short-time locally observable as long as (T_{11}, T_{22}, T_{12}) satisfies

$$4Pe^3 + 4Pe\lambda\nu(T_{11} - T_{22}) - 16\nu(\nu^2 T_{11} T_{22} + Pe^2)T_{12} + 8\nu^2 Pe(T_{11} - T_{22})T_{22} + 8\nu^3 T_{12}(T_{11}^2 + T_{22}^2) \neq 0.$$

Finally, we point out that all of the four models have observability for all stress components almost everywhere under shear flow. In contrast, under extensional flow most of the models have no observability for the shear stress component.

Acknowledgment

This research was supported in part by the Air Force Office of Scientific Research grant F1ATA06313G003, the Army Research Office and the National Science Foundation. The authors thank the anonymous referees for their constructive suggestions on improving this manuscript. The authors also thank Qi Gong for helpful discussions on UKF.

Appendix A. The unscented Kalman filtering

For systems with observability, Kalman filter is a widely used tool to estimate the states using observation data. In this appendix we give a short discussion on the unscented Kalman filtering (UKF) whereas a detailed description of the extended Kalman filtering (EKF) can be found in [8].

Consider a system with output

$$\begin{aligned} \dot{x} &= f(x), \quad x \in \mathbb{R}^n \\ y &= h(x), \quad y \in \mathbb{R}^p \end{aligned} \quad (48)$$

The primary goal of Kalman filter is to estimate the unknown state x using the observation data of y . The initial guess or estimate of x is treated as a random variable with zero mean and a covariance matrix. It can be shown that without sensor error, the estimate, \hat{x} , from Kalman filter asymptotically approaches the accurate value of x . In the presence of noise, the Kalman filter is able to optimize the estimate process by finding the estimate with smallest error (i.e. error with smallest standard deviation).

Like the EKF, the UKF is derived by adding driving and observation noises to the above observed system. In the UKF, it is assumed that the estimate state \hat{x} is always a normally distributed variable at every sampling instance. The mean and covariance information of this random variable can be stored in a set of specially selected sample points called sigma points. These sigma points are easily obtained from the method described in Julier et al. [7]. These sigma points are then propagated through the nonlinear dynamics,

from which the mean and covariance of the estimate can be recovered. UKF is a filter where the true mean and covariance can be more accurately approximated. It can be shown that the nonlinear transformation of the sigma points preserves statistics up to second order in a Taylor series expansion. Based on this fact, a prediction of the state and the covariance matrices in the filter algorithm can be carried out as follows:

- From the previous estimate of the state, \hat{x}_{k-1} , and the covariance matrix, \hat{P}_{k-1}^{xx} , calculate a set of sigma points as

$$\{\hat{x}_{k-1}, \hat{x}_{k-1} \pm (\sqrt{n\hat{P}_{k-1}^{xx}})_i\}; \quad i = 1, 2, \dots, n,$$

where $(\cdot)_i$ is the i th column. A sigma point is denoted by σ^i , $i = 0, 1, \dots, 2n$ and $\sigma^0 = \hat{x}_{k-1}$.

- Propagate all the sigma points σ_i through the nonlinear functions for one step size to obtain z^i . Update the output

$$g^i = h(z^i), \quad i = 1, 2, \dots, n.$$

- Calculate the mean (prediction) of the state and output,

$$\begin{aligned} \tilde{x}_k &= \sum_{i=0}^{2n} W_s^i z^i, \\ \tilde{y}_k &= \sum_{i=0}^{2n} W_s^i g^i, \end{aligned}$$

where W_s^i is the weight [7].

- The prediction of the covariance matrices is given by,

$$\begin{aligned} \tilde{P}_k^{xx} &= \sum_{i=0}^{2n} W_c^i (z^i - \tilde{x}_k)(z^i - \tilde{x}_k)^T, \\ \tilde{P}_k^{yy} &= \sum_{i=0}^{2n} W_c^i (g^i - \tilde{y}_k)(g^i - \tilde{y}_k)^T, \\ \tilde{P}_k^{xy} &= \sum_{i=0}^{2n} W_c^i (z^i - \tilde{x}_k)(g^i - \tilde{y}_k)^T, \end{aligned}$$

where W_c^i is the weight for covariance matrices [7]. Here \tilde{P}_k^{xx} is the covariance matrix of the state and \tilde{P}_k^{yy} is the measurement noise covariance matrix.

- Use the predicted value of \tilde{x}_k , \tilde{P}_k^{xx} , \tilde{P}_k^{yy} and \tilde{P}_k^{xy} to update the estimations as follows

$$\begin{aligned} \hat{x}_k &= \tilde{x}_k + K_k(y_k - \tilde{y}_k). \\ \hat{P}_k^{xx} &= \tilde{P}_k^{xx} - K_k \tilde{P}_k^{yy} K_k^T, \end{aligned}$$

where K_k is the Kalman gain and its value is given by

$$K_k = \tilde{P}_k^{xy} [\tilde{P}_k^{yy}]^{-1}. \quad (49)$$

For a complete description of the unscented Kalman filtering, we refer the readers to the paper by Julier et al. [7].

References

- [1] D.G. Baird, First normal stress difference measurements for polymer melts at high shear rates in a slit-die using hole and exit pressure data, *J. Non-Newtonian Fluid Mech.* 148 (2008) 13–23.
- [2] R.B. Bird, R.C. Armstrong, O. Hassager, *Dynamics of Polymeric Liquids*, 2nd edition, Wiley, 1987.

- [3] F. Fried, C.R. Leal, M.H. Godinho, A.F. Martins, The first normal stress difference and viscosity in shear of liquid crystalline solutions of hydroxypropylcellulose: new experimental data and theory, *Polym. Adv. Technol.* 5 (1994) 596–599.
- [4] R.R. Hermann, A. Krener, Nonlinear controllability and observability, *IEEE Trans. Auto. Control* 22 (1977) 728–740.
- [5] A. Isidori, *Nonlinear Control Systems*, 3rd edition, Springer, 1995.
- [6] A.I. Jomha, P.A. Reynolds, An experimental study of the first normal stress difference—shear stress relationship in simple shear flow for concentrated shear thickening suspensions, *Rheol. Acta* 32 (1993) 457–464.
- [7] S.J. Julier, J.K. Uhlmann, H.F. Durrant-Whyte, A new approach for filtering nonlinear systems, *Proc. Am. Control Conf.* (1995) 1628–1632.
- [8] A. Krener, Eulerian and Lagrangian observability of point vortex flows, *Tellus* 60A (2008) 1089–1102.
- [9] R.G. Larson, *The Structure and Rheology of Complex Fluids*, Oxford, 1998.
- [10] S.E. Mall-Gleissle, W. Gleissle, G.H. McKinley, H. Buggisch, The normal stress behaviour of suspensions with viscoelastic matrix fluids, *Rheol. Acta* 41 (2002) 61–76.
- [11] H. Nijmeijer, A.J. van der Schaft, *Nonlinear Dynamical Control Systems*, Springer, 1990.
- [12] M. Renardy, Are viscoelastic flows under control or out of control? *Syst. Control Lett.* 54 (2005) 1183–1193.
- [13] M. Renardy, Shear flow of viscoelastic fluids as a control problem, *J. Non-Newtonian Fluid Mech.* 131 (2005) 59–63.
- [14] M. Renardy, On control of shear flow of an upper convected Maxwell fluid, *Z. Angew. Math. Mech.* 87 (2007) 213–218.
- [15] L. Wilson, H. Zhou, W. Kang, H. Wang, Controllability of non-Newtonian fluids under homogeneous extensional flow, *Appl. Math. Sci.* 2 (2008) 2145–2156.
- [16] H. Zhou, W. Kang, A. Krener, H. Wang, Homogeneous flow field effect on the control of Maxwell materials, *J. Non-Newtonian Fluid Mech.* 150 (2008) 104–115.